mathematics

MDPI

Article

Fast High-Order Algorithms for Electromagnetic Scattering Problem from Finite Array of Cavities in TE Case with High Wave Numbers

Meiling Zhao [1,*,†], Jiahui He [1,†] and Na Zhu [2,†]

[1] Department of Mathematics and Physics, North China Electric Power University, Baoding 071000, China
[2] School of Mathematics, Shandong University, Jinan 250100, China
* Correspondence: meilingzhao@sina.com
† These authors contributed equally to this work.

Abstract: In this paper, fast high-order finite difference algorithms for solving the electromagnetic scattering from the finite array of two-dimensional rectangular cavities are proposed in TE polarization. The scattering problem from the cavity array is described as coupled Helmholtz equations with transparent boundary conditions on open apertures. Second-order and fourth-order schemes for solving the coupled systems are developed in TE polarization respectively. A special technique is applied to construct a fourth-order scheme for transparent boundary conditions. Further, we propose fast algorithms which can simplify the larger global system to a small linear interface system on the apertures of cavities. Numerical experiments show the validity and efficiency of the proposed fast algorithms for solving the scattering problem with high wave numbers.

Keywords: cavity scattering; fast high order; TE polarization; finite difference

MSC: 65N06; 78M20

check for updates

Citation: Zhao, M.; He, J.; Zhu, N. Fast High-Order Algorithms for Electromagnetic Scattering Problem from Finite Array of Cavities in TE Case with High Wave Numbers. *Mathematics* **2022**, *10*, 2937. https://doi.org/10.3390/math10162937

Received: 18 July 2022
Accepted: 10 August 2022
Published: 15 August 2022

1. Introduction

Electromagnetic scattering from the finite array of large cavities has attracted much attention in industry and the military. The cavity structures are very common, such as jet engine inlet ducts, exhaust nozzles, and cavity-backed antennas. The radar cross section (RCS) is one of the physical parameters of interest, which measures the detectability of a target by a radar system. The accurate prediction of the RCS of the cavities is significant due to its dominance of the overall RCS of the targets.

Numerous works have been devoted to solving the scattering problems from cavities, such as the method of moment (MoM) [1,2], finite element-boundary integral (FE-BI) method [3–8], the finite difference method (FDM) [9–14], and other methods [15–24]. The cavity scattering problems arouse a wide discussion in computational mathematics. Ammari et al. [25,26] gave the result of the existence and uniqueness of the solution to the cavity scattering problem. More mathematical analysis for the cavity scattering problem can be found in [10,25,27].

Most of the studies above were used to solve the electromagnetic scattering from the single cavity model, which limits the practical applications of the model problem in industry and the military. More recently, the finite array of cavity scattering problem was examined in [8,28,29]. Alavikia and Ramahi [8] presented a hybrid finite element boundary integral algorithm to solve the problem of scattering from a finite array of cavities. Li and Wood [28] applied the finite element method to solve the electromagnetic scattering from multiple cavities. Wu and Zheng [29] proposed a perfectly matched layer (PML) method for solving the electromagnetic scattering from multiple cavities. Unfortunately, when the wave number k_0 is high, or the size of the cavity is large compared to the wavelength of the incident wave, the scale of the system will become larger, the computational cost will increase, and the condition number of the matrix will become worse. This has been a crucial topic in the scattering problem for large cavities. A straightforward change of coordinates yields the equivalence of high wave numbers and large cavity problems. For the electromagnetic scattering with high wave numbers, Bao and Sun [10] proposed a fast algorithm for solving the electromagnetic scattering from a large rectangular open cavity in TM polarization.

This paper mainly focuses on the scattering from a finite array of two-dimensional rectangular cavities in TE polarization. In the existing literature or research, the electromagnetic scattering problems in TM polarization have been studied in detail while those in the TE case are seldom discussed. In the TE case, the electric field is perpendicular to the invariant direction. The main difficulty of the scattering from the array of cavities is the complex interaction boundary conditions. In this paper, firstly, by introducing a new transparent boundary condition on the cavity apertures, the finite array of cavity scattering problem is reduced to a boundary value problem of the two-dimensional Helmholtz equation. Considering the boundary coupling of the finite array of cavities, we make extensions of the total field on the apertures. We develop the compact second and fourth-order finite difference schemes respectively to discretize the reduced Helmholtz equation in TE polarization. Moreover, the Neumann boundary condition on the boundaries and the transparent boundary conditions on the apertures need a special approximation. In particular, in order to deal with the problem with high wave numbers, we introduce the discrete Fourier transformation in the horizontal (x-axis) and a Gaussian elimination in the vertical direction (y-axis) on Cartesian coordinates, which can simplify the cavity scattering problem to a small aperture system. Thus the cost of calculating the radar cross section is $O(NM\log(nM))$ with $M \times N$ meshes in each cavity, where n is the number of separate cavities.

The rest of the paper is organized as follows. In Section 2, we illustrate the model problem for the scattering from a single cavity in TE polarization. In Section 3, the compact second-order and fourth-order finite difference schemes are applied to discretize the magnetic field equation in TE polarization. In Section 4, we propose a fast algorithm for the electromagnetic scattering from the finite array of cavities with high wave numbers in TE polarization. Numerical results demonstrate the accuracy and efficiency of the proposed method in Section 5.

2. The Single Cavity Scattering Problem in TE Polarization

We consider an electromagnetic plane wave on a cavity embedded in an infinite ground plane. The total electric field and the magnetic field, denoted by $\mathbf{E}$ and $\mathbf{H}$ separately, satisfy the following time-harmonic Maxwell's equations

$$\nabla \times \mathbf{E} = \mathrm{i}\omega\mathbf{B},$$
$$\nabla \times \mathbf{H} = -\mathrm{i}\omega\mathbf{D},$$

and the constitutive relationship

$$\mathbf{D} = \varepsilon_0\varepsilon_r\mathbf{E},$$
$$\mathbf{B} = \mu_0\mu_r\mathbf{H},$$

where $\varepsilon_0 = 8.85 \times 10^{12}\ \mathrm{Fm}^{-1}$, $\mu_0 = 4\pi \times 10^{-7}\ \mathrm{Hm}^{-1}$, ε_r, μ_r are the relative electric permittivity and magnetic permeability, and $\mathrm{i} = \sqrt{-1}$ and ω is the angular frequency.

For the electromagnetic scattering problem in TE polarization, the electric field is transverse to the z-axis. The magnetic field $\mathbf{H}$ is in the form of $\mathbf{H} = (0, 0, H_z)$. For ease of notation, we denote H_z by u. Let the incident field take the form of $u^i = e^{\mathrm{i}(\alpha x+\beta y)}$, the scattered magnetic field can be expressed by

$$u^s = u - u^i - u^r, \tag{1}$$

where $u^r = e^{\mathrm{i}(\alpha x - \beta y)}$, $\alpha = k_0 \sin\theta$, $\beta = k_0 \cos\theta$, $-\frac{\pi}{2} < \theta < \frac{\pi}{2}$ is the angle of the incidence, k_0 is the wave number in free space.

We consider the cavity filled with a homogeneous medium. The geometry of the cavity is shown in Figure 1. We assume the ground plane Γ^c and the wall S of the cavity are perfect electric conductors (PEC). Denote the upper half space as $\mathbb{R}^2_+ = \{(x,y) \in R^2, y > 0\}$. There exists a homogeneous medium of ε_0 and μ_0 in $\mathbb{R}^2_+$. Therefore, the total magnetic field in the z-axis satisfies the following equations

$$\begin{aligned} &\frac{1}{\varepsilon_r}\triangle u + k_0^2 \mu_r u = 0, && \text{in } \Omega \cup \mathbb{R}^2_+, \\ &\frac{1}{\varepsilon_r}\frac{\partial u}{\partial n} = 0, && \text{on } (\partial\Omega \backslash \Gamma) \cup \Gamma^c, \end{aligned} \tag{2}$$

Together with the Sommerfeld radiation boundary condition

$$\lim_{r \longrightarrow \infty} \sqrt{r}\left(\frac{\partial u^s}{\partial r} - \mathrm{i}k_0 u^s\right) = 0, \tag{3}$$

where $\varepsilon_r = \mu_r = 1$ in R^2_+.

According to Equations (1)–(3), the scattered field u^s satisfies

$$\Delta u^s + k_0^2 u^s = 0, \qquad (x,y) \in \mathbb{R}^2_+, \tag{4}$$

$$\frac{\partial u^s}{\partial n} = 0, \qquad \text{on } \Gamma^c, \tag{5}$$

$$\frac{\partial u^s}{\partial n} = \frac{\partial u}{\partial n}, \qquad \text{on } \Gamma. \tag{6}$$

In order to convert the problem (2) and (3) into the bounded domain, we adopt the upper half-space Neumann Green function for the Helmholtz equation

$$G_N(\boldsymbol{x}, \boldsymbol{x}') = \frac{\mathrm{i}}{4}\left(\mathrm{H}_0^{(1)}(k_0 r) + \mathrm{H}_0^{(1)}(k_0 \bar{r})\right), \tag{7}$$

where $\boldsymbol{x} = (x,y)$, $\boldsymbol{x}' = (x', y')$, $r = \mid \boldsymbol{x} - \boldsymbol{x}' \mid$, $\bar{r} = \mid \boldsymbol{x} - \bar{\boldsymbol{x}}' \mid$, $\bar{\boldsymbol{x}}' = (x', -y')$ and $\mathrm{H}_0^{(1)}$ is the 0-th Hankel function of the first kind.

Green's function (7) satisfies the following equations

$$\triangle G_N + k_0^2 \mu_r G_N = -\delta(\mathbf{x}, \mathbf{x}'), \quad \mathbf{x}, \mathbf{x}' \in \mathbb{R}^2_+, \tag{8}$$

$$\frac{\partial G_N}{\partial n} = 0, \qquad y' = 0 \tag{9}$$

and the Sommerfeld radiation condition

$$\lim_{r \to \infty} \sqrt{r}\left(\frac{\partial G_N}{\partial r} - \mathrm{i}k_0 G_N\right) = 0,$$

where δ is the Dirac delta function.

Multiplying G_N on Equation (4) and u^s on Equation (8), we can derive an equation for G_N and u^s

$$\iint_{\Omega_r^+} (G_N \triangle u^s - u^s \triangle G_N) d\Omega = \iint_{\Omega_r^+} u^s \delta(\boldsymbol{x}, \boldsymbol{x}') d\Omega\,. \tag{10}$$

According to the property of $\delta-$function and Green's formulation, we have

$$u^s(\mathbf{x}) = \int_\Gamma \left(G_N(\mathbf{x}', \mathbf{x}) \frac{\partial u^s(\mathbf{x}')}{\partial n(\mathbf{x}')} - u^s(\mathbf{x}') \frac{\partial G_N(\mathbf{x}', \mathbf{x})}{\partial n(\mathbf{x}')}\right) ds(\mathbf{x}'). \tag{11}$$

A detailed derivation is available in [3].

In terms of Equations (5) and (9), the above equation can be written as

$$u^s(\boldsymbol{x}) = \int_\Gamma \left[G_N(\boldsymbol{x}', \boldsymbol{x}) \frac{\partial u^s(\boldsymbol{x}')}{\partial n(\boldsymbol{x}')} \right]_{y'=0^+} ds(\boldsymbol{x}') = -\int_\Gamma \left[G_N(\boldsymbol{x}', \boldsymbol{x}) \frac{\partial u^s(\boldsymbol{x}')}{\partial y'} \right]_{y'=0^+} dx'. \tag{12}$$

Substituting Equations (1) and (7) into the above equation, we obtain

$$u(x) = 2e^{\mathrm{i}\alpha x} - \frac{\mathrm{i}}{2} \int_\Gamma H_0^{(1)}(k_0 \mid x - x' \mid) \frac{\partial u(x')}{\partial y'} dx',$$

where $H_0^{(1)}(v) = J_0(v) + \mathrm{i}Y_0(v)$. $J_0(v), Y_0(v)$ are Bessel functions of the first and second kinds of order 0 respectively.

Noting the continuity conditions on the aperture Γ

$$u(x,y) \mid_{y=0^+} = u(x,y) \mid_{y=0^-}, \frac{\partial u}{\partial n} \mid_{y=0^+} = \frac{1}{\varepsilon_r} \frac{\partial u}{\partial n} \mid_{y=0^-},$$

We can obtain the transparent boundary on Γ

$$u(x) = 2e^{\mathrm{i}\alpha x} - \frac{\mathrm{i}}{2} \int_\Gamma H_0^{(1)}(k_0 \mid x - x' \mid) \frac{1}{\varepsilon_r} \frac{\partial u(x')}{\partial y'} \mid_{y'=0^-} dx'.$$

Let $g(x) = 2e^{\mathrm{i}\alpha x}$, the transparent boundary condition on Γ in TE polarization can be simplified as

$$u = \mathbb{T}\left(\frac{1}{\varepsilon_r} \frac{\partial u}{\partial y} \right) + g(x), \tag{13}$$

where $\mathbb{T}\left(\frac{1}{\varepsilon_r} \frac{\partial u}{\partial y} \right) = -\frac{\mathrm{i}}{2} \int_\Gamma H_0^{(1)}(k_0 \mid x - x' \mid) \frac{1}{\varepsilon_r} \frac{\partial u(x')}{\partial y'} \mid_{y'=0^-} dx'$.

Hence, the electromagnetic scattering from the single cavity in TE polarization can be transformed into the following equations in a bounded domain [28].

$$\begin{cases} \nabla \cdot \left(\dfrac{1}{\varepsilon_r} \nabla u \right) + k_0^2 \mu_r u = 0, & \text{in } \Omega, \\ \dfrac{1}{\varepsilon_r} \dfrac{\partial u}{\partial n} = 0, & \text{on } (\partial\Omega \backslash \Gamma) \cup \Gamma^c, \\ u = \mathbb{T}\left(\dfrac{1}{\varepsilon_r} \dfrac{\partial u}{\partial n} \right) + g(x), & \text{on } \Gamma. \end{cases} \tag{14}$$

The existence and uniqueness of solutions of (14) for arbitrary wave numbers have been obtained in [26].

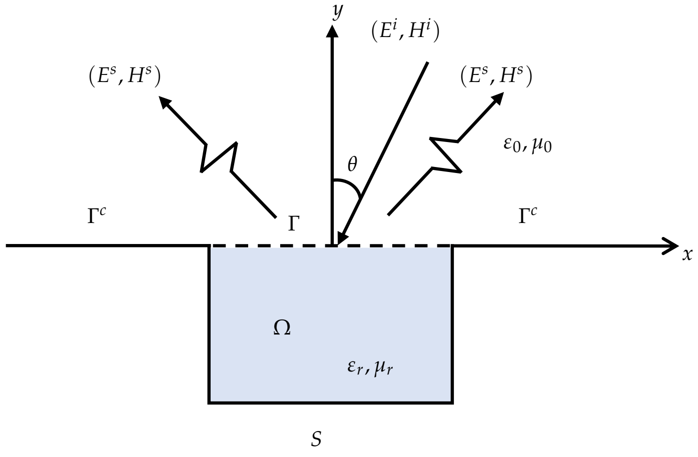

Figure 1. Single cavity scattering geometry.

3. Fast High-Order Schemes for the Scattering from Single Cavity

3.1. Second-Order Finite Difference Scheme

Let $\{x_i, y_j\}_{i,j=0}^{M+1,N+1}$ define a uniform partition on $\Omega = [0,a] \times [-b,0]$ with $x_i = ih_x$, $i = 0,1,\ldots,M+1$, $y_j = -b + jh_y, j = 0,1,\ldots,N+1$, $h_x = a/(M+1)$, $h_y = b/(N+1)$. For simplicity, we consider the case of $h_x = h_y = h$. It can be generalized to the case of $h_x \neq h_y$. Denote $u_{i,j}$ as the numerical solution at point (x_i, y_j). The second-order finite difference approximation inside the cavity can be written as

$$\frac{1}{\varepsilon_r}\left(\delta_x^2 + \delta_y^2\right)u_{i,j} + k_0^2\mu_r u_{i,j} = f_{i,j},\ i = 0,1,\ldots,M+1, j = 0,1,\ldots,N+1, \tag{15}$$

where δ_x^2, δ_y^2 are second-order finite difference operators.

Considering the second-order approximation for Neumann boundary condition on $y = -b$

$$\frac{u_{i,1} - u_{i,-1}}{2h} = \frac{\partial u}{\partial n}\mid_{y=-b} + O(h^2).$$

Since $\frac{\partial u}{\partial n} = 0$, we have $u_{i,-1} = u_{i,1}, i = 0,1,\ldots,M+1$. The Neumann boundary conditions on the left and right boundaries can be handled analogously.

Denote all the unknowns by:

$$U = (u_{0,0}, u_{0,1}, \ldots, u_{0,N}, u_{1,0}, u_{1,1}, \ldots, u_{1,N}, \ldots, u_{M+1,0}, u_{M+1,1}, \ldots, u_{M+1,N}),$$
$$u_{N+1} = (u_{0,N+1}, u_{1,N+1}, \ldots, u_{M+1,N+1}).$$

Therefore, we can rewrite the second-order scheme (15) as the matrix form

$$\left(\frac{1}{\varepsilon_r}(A_x \otimes I_{N+1} + I_{M+2} \otimes A_y) + k_0^2\mu_r I\right)U + \frac{1}{\varepsilon_r}(I_{M+2} \otimes a_{N+1})u_{:,N+1} = F, \tag{16}$$

where

$$A_x = \frac{1}{h^2}\begin{pmatrix} -2 & 2 & & & \\ 1 & -2 & 1 & & \\ & \ddots & \ddots & \ddots & \\ & & 1 & -2 & 1 \\ & & & 2 & -2 \end{pmatrix}, \quad A_y = \frac{1}{h^2}\begin{pmatrix} -2 & 2 & & & \\ 1 & -2 & 1 & & \\ & \ddots & \ddots & \ddots & \\ & & 1 & -2 & 1 \\ & & & 1 & -2 \end{pmatrix},$$

$$a_{N+1} = \frac{1}{h^2}(0,\ldots,0,1)^T,$$
$$F = (f_{0,0}, f_{0,1}, \ldots, f_{0,N}, f_{1,0}, f_{1,1}, \ldots, f_{1,N}, \ldots, f_{M+1,0}, f_{M+1,1}, \ldots, f_{M+1,N})^T.$$

Here $\otimes$ is the Kronecker product. I_{M+2} and I_{N+1} are identity matrix in $(M+2) \times (M+2)$ dimension and $(N+1) \times (N+1)$ dimensions respectively, I is identity matrix in $(M+2)(N+1) \times (M+2)(N+1)$ dimensions.

Below we consider the approximations of the transparent boundary in (13). The nonlocal integral operator in (13) can be rewritten by

$$\begin{aligned}\mathbb{T}\left(\frac{\partial u}{\partial y}\right) =& \frac{1}{2}\int_\Gamma Y_0(k_0 \mid x - x' \mid)\frac{\partial u(x')}{\partial y'}\mid_{y'=0^-} dx' \\ & - \frac{\mathrm{i}}{2}\int_\Gamma J_0(k_0 \mid x - x' \mid)\frac{\partial u(x')}{\partial y'}\mid_{y'=0^-} dx'.\end{aligned} \tag{17}$$

Since $Y_0(v) \sim \frac{2}{\pi}\ln\frac{v}{2}$ as $v \to 0$, the first part of Equation (17) contains the weakly singular integral.

We adopt a piecewise linear approximation for the first item and a trapezoidal formulation for the second item of Equation (17). So the nonlocal integral operator $\mathbb{T}(z)$ can be approximated as follows

$$\mathbb{T}(z) \approx \sum_{j=1}^{M} T_{ij} z_j,$$

where

$$\begin{aligned}
T_{ij} &= T_{ij}^{\mathrm{re}} + \mathrm{i} T_{ij}^{\mathrm{im}}, \\
T_{ij}^{\mathrm{re}} &= \frac{1}{2} \int_{\Gamma} Y_0(k_0 \mid x_i - x_j \mid) \phi_j^1(x') dx', \\
T_{ij}^{\mathrm{im}} &= -\frac{h}{2} J_0(k_0 \mid x_i - x_j \mid),
\end{aligned}$$

and $\phi_j^1(x')$ are the piecewise linear basis functions.

The second-order approximation for (13) is given as

$$u_{:,N+1} = T \frac{1}{\varepsilon_r} \frac{u_{:,N+2} - u_{:,N}}{2h} + g(x_{:,N+1}). \tag{18}$$

Moreover, $u_{:,N+1}$ satisfies the second-order scheme (15)

$$\frac{1}{\varepsilon_r} \left(\delta_x^2 + \delta_y^2 \right) u_{i,N+1} + k_0^2 u_{i,N+1} = f_{i,N+1}, i = 0, 1, \ldots, M+1. \tag{19}$$

Rewrite (19) into matrix form [10].

$$\left(\frac{1}{\varepsilon_r} \left(A_x - \frac{2}{h^2} I_{M+2} \right) + k_0^2 \right) u_{:,N+1} + \frac{1}{\varepsilon_r h^2} u_{:,N} + \frac{1}{\varepsilon_r h^2} u_{:,N+2} = F_{:,N+1}. \tag{20}$$

Combining (18) and (20), we have

$$2T u_{:,N} + (2h\varepsilon_r I_{M+2} + T J_2^{-1} J_1) u_{:,N+1} = T J_2^{-1} F_{:,N+1} + 2h\varepsilon_r g, \tag{21}$$

where $J_1 = \frac{1}{\varepsilon_r}\left(A_x - \frac{2}{h^2} I_{M+2} \right) + k_0^2 I_{M+2}$, $J_2 = \frac{1}{\varepsilon_r h^2} I_{M+2}$.

Then we derive the reduced linear system

$$\begin{pmatrix} A_{11} & A_{12} \\ A_{21} & A_{22} \end{pmatrix} \begin{pmatrix} U \\ u_{:,N+1} \end{pmatrix} = \begin{pmatrix} F \\ F_\Gamma \end{pmatrix},$$

where

$$\begin{aligned}
A_{11} &= \frac{1}{\varepsilon_r} (A_x \otimes I_{N+1} + I_{M+2} \otimes A_y) + k_0^2 \mu_r I, \\
A_{12} &= \frac{1}{\varepsilon_r} (I_{M+2} \otimes a_{N+1}), \\
A_{21} &= 2T \otimes a_{N+1}^T, \quad A_{22} = 2h\varepsilon_r I_{M+2} + T J_2^{-1} J_1, \\
F_\Gamma &= T J_2^{-1} F_{:,N+1} + 2h\varepsilon_r g.
\end{aligned}$$

3.2. The Fast Second-Order Algorithm for the Scattering from the Single Cavity

For the matrix A_x, we have

$$C_x^{-1} A_x C_x = \Lambda = \mathrm{diag}(\lambda_1, \lambda_2, \ldots, \lambda_{M+2}),$$

where C_x is the discrete cosine transformation matrix,

$$(C_x)_{ij} = \cos \frac{\pi i j}{M+1}, \lambda_i = 2\cos\left(\frac{i\pi}{M+1} \right) - 2, \quad i, j = 0, 1, 2, \ldots, M+1.$$

Multiplying $C_x^{-1} \otimes I_{N+1}$ on both sides of Equation (16), we have

$$\frac{1}{\varepsilon_r}(\Lambda \otimes I_{N+1} + I_{M+2} \otimes A_y)\bar{U} + k_0^2\mu_r\bar{U} + \frac{1}{\varepsilon_r}(I_{M+2} \otimes a_{N+1})\bar{u}_{:,N+1} = \bar{F}, \tag{22}$$

where

$$\begin{aligned}
&\bar{U} = (C_x^{-1} \otimes I_{N+1})u \\
=&(\bar{u}_{0,0}, \bar{u}_{0,1}, \cdots, \bar{u}_{0,N}, \bar{u}_{1,0}, \bar{u}_{1,1}, \cdots, \bar{u}_{1,N}, \cdots, \bar{u}_{M+1,0}, \bar{u}_{M+1,1}, \cdots, \bar{u}_{M+1,N})^T, \\
&\bar{F} = (C_x^{-1} \otimes I_{N+1})F \\
=&(\bar{f}_{0,0}, \bar{f}_{0,1}, \cdots, \bar{f}_{0,N}, \bar{f}_{10}, \bar{f}_{11}, \cdots, \bar{f}_{1N}, \cdots, \bar{f}_{M+1,0}, \bar{f}_{M+1,1}, \cdots, \bar{f}_{M+1,N})^T. \\
&\bar{u}_{:,N+1} = C_x^{-1}u_{:,N+1} = (\bar{u}_{0,N+1}, \bar{u}_{1,N+1}, \cdots, \bar{u}_{M+1,N+1})^T,
\end{aligned}$$

Moreover, Equation (22) can be written as $M+2$ systems

$$\left(\frac{1}{\varepsilon_r}(\lambda_i I_{N+1} + A_y) + k_0^2\mu_r I_{N+1}\right)\bar{U}_{i,:} + \frac{1}{\varepsilon_r}a_{N+1}\bar{u}_{i,N+1} = \bar{F}_{i,:},\ i = 0,1,\cdots,M+1, \tag{23}$$

where

$$\bar{U}_{i,:} = (\bar{u}_{i,0}, \bar{u}_{i,1}, \ldots, \bar{u}_{i,N})^T, \bar{F}_{i,:} = (\bar{f}_{i,0}, \bar{f}_{i,1}, \ldots, \bar{f}_{i,N})^T.$$

As can be seen from Equation (23), $\frac{1}{\varepsilon_r}(\lambda_i I_{N+1} + A_y) + k_0^2\mu_r I_{N+1}$ is a tridiagonal matrix. For small enough h, we can derive the LU decomposition

$$\frac{1}{\varepsilon_r}(\lambda_i I_{N+1} + A_y) + k_0^2\mu_r I_{N+1} = \mathbb{L}_i\mathbb{U}_i,\ i = 0,1,2,\ldots,M+1.$$

Multiplying $\mathbb{L}_i^{-1}$ on both sides of Equation (23), we have

$$\mathbb{U}_i\bar{U}_{i,:} + \frac{1}{\varepsilon_r}\mathbb{L}_i^{-1}a_{N+1}\bar{u}_{i,N+1} = \mathbb{L}_i^{-1}\bar{F}_{i,:}\,.$$

Extracting the last elements from the above systems, we can obtain

$$p_i\bar{u}_{i,N} + q_i\bar{U}_{i,N+1} = \tilde{f}_{i,N},\ i = 0,1,\ldots,M+1,$$

where p_i and q_i are the last elements of $\mathbb{U}_i$ and $\mathbb{L}_i^{-1}a_{N+1}/\varepsilon_r$ respectively, and $\tilde{f}_{i,N}$ is the last element of $\mathbb{L}_i^{-1}\bar{F}_{i,:}$.

For $i = 0,1,\ldots,M+1$, we have

$$P\bar{u}_{:,N} + Q\bar{u}_{:,N+1} = \tilde{F},$$

where $P = \mathrm{diag}(p_1, p_2, \ldots, p_{M+2})$, $Q = \mathrm{diag}(q_1, q_2, \ldots, q_{M+2})$ and $\tilde{F} = (\tilde{f}_{0,N}, \tilde{f}_{1,N}, \ldots, \tilde{f}_{M+1,N})^T$.

Combining with Equation (21), we can derive the reduced formulation only with the unknowns on the aperture

$$\left(2h\varepsilon_r C_x + TC_xJ_2^{-1}J_1 - 2TC_xP^{-1}Q\right)\bar{u}_{:,N+1} = 2h\varepsilon_r g + TC_xJ_2^{-1}\bar{F}_{:,N+1} - 2TC_xP^{-1}\tilde{F}. \tag{24}$$

We analyze the computational cost of Algorithm 1. The matrix T is calculated by using the traditional trapezoidal formula, and the cost of Step (i) is $O(M+2)$. In Step (ii), we need to calculate the LU-decomposition for $(\lambda_i I_{N+1} + A_y)/\varepsilon_r + k_0^2 I_{N+1}$. Noting the tridiagonal structure of these matrices, we only need $O((M+2)(N+1))$ operations if $f \neq 0$. The cost of calculating the product of the matrix C_x and a complex vector is $O((M+2)^2(N+1))$ in Step (iii). In Step (iv), we use the BiCG method for solving the linear systems (24). Each iteration only needs to calculate one matrix-vector multiplication, and the cost of each iteration is $O(24p(M+2)\log(M+2))$, p is the number of iterations.

Algorithm 1: The procedure of the second-order fast algorithm for scattering from the single cavity (The Fast Algorithm for the Scattering Problem From the Single Cavity).

Step (i)	Generate the matrix T.
Step (ii)	Calculate the LU decomposition to get P and Q by using the forward Gaussian elimination with a row partial pivoting.
Step (iii)	Calculate $C_x F$.
Step (iv)	Solve the system (24) for $\bar{u}_{:,N+1}$.
Step (v)	Solve the system (22) for rest of the unknowns.

3.3. Fourth-Order Finite Difference Scheme

The fourth-order compact finite difference scheme can be written as

$$\left(\frac{1}{\varepsilon_r}+\frac{k^2h^2}{12}\right)\left(\delta_x^2+\delta_y^2\right)u_{i,j}+\frac{h^2}{6}\frac{1}{\varepsilon_r}\delta_x^2\delta_y^2u_{i,j}+k_0^2u_{i,j}=f_{i,j}+\frac{h^2}{12}\Delta f_{i,j}, \quad i=0,1,\dots,M+1, j=0,1,\dots,N+1. \tag{25}$$

$E_{i,j}$ is the leading truncation error and is given by

$$\begin{aligned} E_{i,j}=&\left(\frac{k^2}{144}\left(u_{x^4}+u_{y^4}\right)_{i,j}+\frac{1}{360\varepsilon_r}\left(u_{x^6}+u_{y^6}\right)_{i,j}+\frac{1}{72\varepsilon_r}\left(u_{x^4y^2}+u_{x^2y^4}\right)_{i,j}\right)h^4 \\ &-\left(\frac{1}{144}\left(f_{x^4}+f_{y^4}\right)_{i,j}\right)h^4. \end{aligned}$$

Otherwise, Equation (25) can be written as

$$\begin{aligned} &c_2u_{i-1,j-1}+c_1u_{i-1,j}+c_2u_{i-1,j+1}+c_1u_{i,j-1}+c_0u_{i,j}+c_1u_{i,j+1} \\ &+c_2u_{i+1,j-1}+c_1u_{i+1,j}+c_2u_{i+1,j+1}=F_{i,j}, \end{aligned} \tag{26}$$

where $c_0=\frac{2k^2h^2}{3}-\frac{10}{3\varepsilon_r}$, $c_1=\frac{k^2h^2}{12}+\frac{2}{3\varepsilon_r}$, $c_2=\frac{1}{6\varepsilon_r}$, $F_{i,j}=h^2f_{i,j}+\frac{h^4}{12}\Delta f_{i,j}$.

Next, we consider the Neumann boundary condition on the boundary S. By Taylor's expansion, we can obtain the fourth-order approximation for $\frac{\partial u}{\partial n}=0$ on $y=-b$

$$\frac{\partial u}{\partial y}\mid_{y=-b}=\frac{u_{i,1}-u_{i,-1}}{2h}-\frac{h^2}{6}\left(u_{yyy}\right)_{i,0}+O\left(h^4\right).$$

Since $\frac{\partial u}{\partial y}\mid_{y=-b}=0$ and $u_{yyy}=\varepsilon_r f_y-k^2\varepsilon_r u_y-u_{xxy}$, we have

$$\left(\frac{1}{\varepsilon_r}+\frac{h^2k^2}{6}+\frac{h^2}{6\varepsilon_r}\delta_x^2\right)u_{i,1}-\left(\frac{h^2k^2}{6\varepsilon_r}+\frac{h^2}{6\varepsilon_r}\delta_x^2\right)u_{i,-1}=\frac{h^3}{3}(f_y)_{i,0}, \quad i=0,1,\dots,M+1. \tag{27}$$

Moreover, Equation (25) can be written as

$$\begin{aligned} &\left(\frac{1}{\varepsilon_r}+\frac{k^2h^2}{12}+\frac{h^2}{6\varepsilon_r}\delta_x^2\right)u_{i,j+1}+\left(\left(\frac{1}{\varepsilon_r}+\frac{k^2h^2}{12}\right)\left(h^2\delta_x^2-2\right)-\frac{h^2}{3\varepsilon_r}\delta_x^2+k^2h^2\right)u_{i,j} \\ &+\left(\frac{1}{\varepsilon_r}+\frac{k^2h^2}{12}+\frac{h^2}{6\varepsilon_r}\delta_x^2\right)u_{i,j-1} \\ &=h^2f_{i,j}+\frac{h^4}{12}\Delta f_{i,j}, \quad i=0,1,\dots,M+1, j=0,1,\dots,N+1. \end{aligned}$$

Let $j = 0$, we have

$$\begin{aligned}
&\left(\frac{1}{\varepsilon_r} + \frac{k_0^2 h^2}{12} + \frac{h^2}{6\varepsilon_r}\delta_x^2\right)u_{i,1} + \left(\left(\frac{1}{\varepsilon_r} + \frac{k_0^2 h^2}{12}\right)\left(h^2\delta_x^2 - 2\right) - \frac{h^2}{3\varepsilon_r}\delta_x^2 + k_0^2 h^2\right)u_{i,0} \\
&+\left(\frac{1}{\varepsilon_r} + \frac{k_0^2 h^2}{12} + \frac{h^2}{6\varepsilon_r}\delta_x^2\right)u_{i,-1} \\
&= h^2 f_{i,j} + \frac{h^4}{12}\Delta f_{i,j}, \quad i = 0, 1, \ldots, M+1.
\end{aligned} \tag{28}$$

Combining Equations (27) and (28), we have

$$\begin{aligned}
&2\left(\frac{1}{\varepsilon_r} + \frac{k_0^2 h^2}{12} + \frac{h^2}{6\varepsilon_r}\delta_x^2\right)u_{i,1} + \left(\left(\frac{1}{\varepsilon_r} + \frac{k_0^2 h^2}{12}\right)\left(h^2\delta_x^2 - 2\right) - \frac{h^2}{3\varepsilon_r}\delta_x^2 + k_0^2 h^2\right)u_{i,0} \\
&= h^2 f_{i,0} + \frac{h^3}{3}(f_y)_{i,0} + \frac{h^4}{12}\Delta f_{i,0}, \quad i = 0, 1, \ldots, M+1.
\end{aligned}$$

Similarly, we can derive the fourth-order approximation of the Neumann boundary condition on the other side of the boundaries. Therefore, the compact fourth-order scheme can be written as the following matrix form

$$\begin{aligned}
&\left(\left(\frac{1}{\varepsilon_r} + \frac{k^2 h^2}{12}\right)(A_x \otimes I_{N+1} + I_{M+2} \otimes A_y) + \frac{h^2}{6\varepsilon_r}(A_x \otimes A_y) + k^2 I\right)U_1 \\
&+\left(\left(\frac{1}{\varepsilon_r} + \frac{k^2 h^2}{12}\right)(I_{M+2} \otimes a_{N+1}) + \frac{h^2}{6\varepsilon_r}(A_x \otimes a_{N+1})\right)u_{:,N+1} \\
&= F_1 + \frac{h^2}{12}\Delta F_1 + \frac{1}{12}(I_{M+2} \otimes b_{N+1})f_{:,0} + \frac{1}{12}(b_{N+1} \otimes I_{M+2})f_{0,:} \\
&+\frac{1}{12}(a_{N+1} \otimes I_{M+2})f_{M+1,:},
\end{aligned} \tag{29}$$

where

$$F_1 = (f_{0,0}, f_{0,1}, \cdots, f_{0,N}, f_{1,0}, f_{1,1}, \cdots, f_{1,N}, \cdots, f_{M+1,0}, f_{M+1,1}, \cdots, f_{M+1,N})^T,$$

$$U_1 = (u_{0,0}, u_{0,1}, \cdots, u_{0,N}, u_{1,0}, u_{1,1}, \cdots, u_{1,N}, \cdots, u_{M+1,0}, u_{M+1,1}, \cdots, u_{M+1,N}),$$

$$b_{N+1} = \frac{1}{h^2}(1, 0, \cdots, 0)^T.$$

Below we need to deal with the transparent boundary condition on the aperture in particular. Firstly, By means of Taylor's expansion, we have

$$\frac{\partial u}{\partial y} = \frac{u_{i,N+2} - u_{i,N}}{2h} - \frac{h^2}{6}\left(\varepsilon_r f_y - k^2\varepsilon_r u_y - u_{xxy}\right)|_{i,N+1} + O(h^4),\ i = 0, 1, \ldots, M+1.$$

Then in order to eliminate the ghost points, we introduce the variable ν

$$\begin{aligned}
u_y &= \frac{u_{i,N+2} - u_{i,N}}{2h} + \nu h^2 u_{xxy} + O(h^2) \\
&= \frac{(1-2\nu)(u_{i,N+2} - u_{i,N})}{2h} + \frac{\nu(u_{i+1,N+2} + u_{i-1,N+2} - u_{i+1,N} - u_{i-1,N})}{2h}.
\end{aligned}$$

Therefore, we have

$$\begin{aligned}\frac{\partial u}{\partial y} =& \frac{u_{i,N+2}-u_{i,N}}{2h} - \frac{h^2}{6}(\varepsilon_r f_y)_{i,N+1} \\ &+ \frac{1}{6}\frac{(u_{i+1,N+2}-2u_{i,N+2}+u_{i-1,N+2})-(u_{i+1,N}-2u_{i,N}+u_{i-1,N})}{2h} \\ &+ \frac{\varepsilon_r k^2h^2}{6}\left(\frac{(1-2\nu)(u_{i,N+2}-u_{i,N})}{2h} + \frac{\nu(u_{i+1,N+2}+u_{i-1,N+2}-u_{i+1,N}-u_{i-1,N})}{2h}\right).\end{aligned}$$

Combing with the transparent boundary condition (13), we have

$$\begin{aligned}\sum_{l=1}^{M+2}\vartheta_{i,l}u_{l,N+1} - \hat{g}_i + \frac{h^3}{3}(f_y)_{i,N+1} =& \left(\frac{2}{3\varepsilon_r} + \frac{k^2h^2}{6}(1-2\nu)\right)(u_{i,N+2}-u_{i,N}) \\ &+ \left(\frac{1}{6\varepsilon_r} + \nu\frac{k^2h^2}{6}\right)(u_{i+1,N+2}+u_{i-1,N+2}) \\ &- \left(\frac{1}{6\varepsilon_r} + \nu\frac{k^2h^2}{6}\right)(u_{i+1,N}+u_{i-1,N}),\end{aligned} \tag{30}$$

where $\vartheta_{i,l} = 2hT^{-1}_{i,l}, \hat{g}_i = 2h\sum_{l=1}^{M+2}T^{-1}_{i,l}g$.

Take $j = N+1$ for the fourth-order scheme (25), we have

$$\begin{aligned}&c_1(u_{i,N+2}+u_{i,N}) + c_2(u_{i+1,N+2}+u_{i-1,N+2}+u_{i+1,N}+u_{i-1,N}) \\ &+ c_1(u_{i+1,N+1}+u_{i-1,N-1}) + c_0u_{i,N+1} \\ =& h^2 f_{:,N+1} + \frac{h^4}{12}\Delta f_{:,N+1}.\end{aligned} \tag{31}$$

Moreover, Equation (30) can be written as

$$\begin{aligned}&\tilde{c}_1(u_{i,N+2}-u_{i,N}) + \tilde{c}_2(u_{i+1,N+2}+u_{i-1,N+2}-u_{i+1,N}-u_{i-1,N}) - \sum_{l=1}^{M+2}\vartheta_{i,l}u_{l,N+1} \\ =& \frac{h^3}{3}(f_y)_{i,N+1} - \hat{g}_i,\end{aligned} \tag{32}$$

where $\tilde{c}_1 = \frac{2}{3\varepsilon_r} + \frac{k^2h^2}{6}(1-2\nu)$, $\tilde{c}_2 = \frac{1}{6\varepsilon_r} + \nu\frac{k^2h^2}{6}$.

To eliminate $u_{i,N+2}, u_{i-1,N+2}, u_{i+1,N+2}$, we define a constant η such that

$$\eta = \frac{c_1}{\tilde{c}_1} = \frac{c_2}{\tilde{c}_2}.$$

We have computed $\nu k^2h^2 = \frac{(\frac{4}{\varepsilon_r}+k^2h^2)c_2 - \frac{1}{\varepsilon_r}c_1}{c_1+2c_2}$, hence

$$\begin{aligned}\tilde{c}_1 &= \left(\frac{1}{\varepsilon_r} + \frac{k^2h^2}{6}\right)\frac{c_1}{c_1+2c_2}, \\ \tilde{c}_2 &= \frac{c_2}{c_1}\tilde{c}_1, \\ \eta &= \left(\frac{1}{\varepsilon_r} + \frac{k^2h^2}{6}\right)^{-1}(c_1+2c_2).\end{aligned}$$

Therefore, combing Equations (26) and (32), the reduced equation can be written as

$$\begin{aligned}
&\eta \sum_{l=1}^{M+2} \vartheta_{i,l} u_{l,N+1} + 2c_1 u_{i,N} + 2c_2(u_{i+1,N} + u_{i-1,N}) \\
&+ c_1(u_{i+1,N+1} + u_{i-1,N+1}) + c_0 u_{i,N+1} \\
=& h^2 f_{:,N+1} + \frac{h^4}{12}\Delta f_{:,N+1} + \eta \hat{g}_i - \eta \frac{h^3}{3}(f_y)_{i,N+1}.
\end{aligned}$$

Denote

$$\begin{aligned}
L_1 &= \left(\frac{1}{\varepsilon_r} + \frac{k^2h^2}{12}\right) I_{M+2} + \frac{h^2}{6\varepsilon_r} A_x, \\
L_2 &= \left(\frac{1}{\varepsilon_r} + \frac{k^2h^2}{12}\right)\left(h^2 A_x - 2I_{M+2}\right) - \frac{h^2}{3\varepsilon_r} A_x + k^2h^2 I_{M+2}.
\end{aligned}$$

The above equation can be written in matrix form

$$\begin{aligned}
&2TL_1 u_{:,N} + (2h\eta I_{M+2} + TL_2) u_{:,N+1} \\
=& 2h\eta g + T\left(h^2 F_{:,N+1} + \frac{h^4}{12}\Delta F_{:,N+1} - \eta \frac{h^3}{3}(f_y)_{:,N+1}\right)
\end{aligned} \tag{33}$$

Then we derive the reduced linear system

$$\begin{pmatrix} A_{11} & A_{12} \\ A_{21} & A_{22} \end{pmatrix} \begin{pmatrix} U \\ u_{:,N+1} \end{pmatrix} = \begin{pmatrix} F \\ F_\Gamma \end{pmatrix}, \tag{34}$$

where

$$\begin{aligned}
A_{11} &= \left(\frac{1}{\varepsilon_r} + \frac{k^2h^2}{12}\right)(A_x \otimes I_N + I_M \otimes A_y) + \frac{h^2}{6}\frac{1}{\varepsilon_r}(A_x \otimes A_y) + k^2 I, \\
A_{12} &= \left(\frac{1}{\varepsilon_r} + \frac{k^2h^2}{12}\right)(I_M \otimes a_{N+1}) + \frac{h^2}{6}\frac{1}{\varepsilon_r}(A_x \otimes a_{N+1}), \\
A_{21} &= 2TL_1 \otimes a_{N+1}^T, \quad A_{22} = 2hI_{M+2} + TL_2, \\
F &= F_1 + \frac{h^2}{12}\Delta F + \frac{h}{3}(\tilde{I}_{M+2} \otimes b_{N+1})(f_y)_{:,0} + \frac{h}{3}(b_{N+1} \otimes I_{M+2})(f_x)_{0,:} \\
&\quad + \frac{h}{3}(a_{N+1} \otimes I_{M+2})(f_x)_{M+1,:}, \\
F_\Gamma &= 2h\eta g + T\left(h^2 F_{:,N+1} + \frac{h^4}{12}\Delta F_{:,N+1} - \eta \frac{h^3}{3}(f_y)_{:,N+1}\right), \\
\tilde{I}_{M+2} &= \mathrm{diag}(0, 1, \ldots, 1, 0).
\end{aligned}$$

3.4. The Fast Fourth-Order Algorithm for the Scattering from the Single Cavity

Multiple $C_x^{-1} \otimes I_{N+1}$ on both side of (29), we have

$$\begin{aligned}
&\left(\left(\frac{1}{\varepsilon_r} + \frac{k^2h^2}{12}\right)(\Lambda \otimes I_{N+1} + I_{M+2} \otimes A_y) + \frac{h^2}{6\varepsilon_r}(\Lambda \otimes A_y) + k^2 I\right)\bar{U}_1 \\
+&\left(\left(\frac{1}{\varepsilon_r} + \frac{k^2h^2}{12}\right)(I_{M+2} \otimes a_{N+1}) + \frac{h^2}{6\varepsilon_r}(A_x \otimes a_{N+1})\right)\bar{u}_{:,N+1} = \bar{F},
\end{aligned}$$

where

$$\bar{F} = \left(C_x^{-1} \otimes I_{N+1}\right)\left(F_1 + \frac{h^2}{12}\Delta F_1 + \frac{1}{12}(I_{M+2} \otimes b_{N+1})f_{:,0} + \frac{1}{12}(b_{N+1} \otimes I_{M+2})f_{0,:}\right)$$
$$+ \left(C_x^{-1} \otimes I_{N+1}\right)\left(\frac{1}{12}(a_{N+1} \otimes I_{M+2})f_{M+1,:}\right).$$

Therefore, we have $M+2$ linear systems which are written as

$$\left(\left(\frac{1}{\varepsilon_r} + \frac{k^2h^2}{12}\right)(\lambda_i I_{N+1} + A_y) + \frac{h^2}{6\varepsilon_r}(\lambda_i A_y) + k_0^2 I_{N+1}\right)\bar{u}_{i,:}$$
$$+ \left(\frac{1}{\varepsilon_r} + \frac{k^2h^2}{12} + \frac{h^2}{6\varepsilon_r}\lambda_i\right)a_{N+1}\bar{u}_{i,N+1} = \bar{F}_{i,:}.$$

Let $\left(\frac{1}{\varepsilon_r} + \frac{k^2h^2}{12}\right)(\lambda_i I_{N+1} + A_y) + \frac{h^2}{6\varepsilon_r}\lambda_i A_y + k_0^2 I_{N+1} = \mathbb{L}_i\mathbb{U}_i$ be the LU-decomposition, for enough small h, we have

$$\mathbb{U}_i\bar{u}_{i,:} + \mathbb{L}_i^{-1}\left(\frac{1}{\varepsilon_r} + \frac{k^2h^2}{12} + \frac{h^2}{6\varepsilon_r}\lambda_i\right)a_{N+1}\bar{u}_{i,N+1} = \mathbb{L}_i^{-1}\bar{F}_{i,:}.$$

Take the last element of the above equation, we have the following relationship between u_N and u_{N+1}

$$\bar{u}_{:,N} = -P^{-1}Q\bar{u}_{:,N+1} + P^{-1}\mathbb{L}_i^{-1}\bar{F}_{:,N}, \tag{35}$$

where $P = \operatorname{diag}(p_1, p_2, \ldots, p_{M+2}), Q = \operatorname{diag}(q_1, q_2, \ldots, q_{M+2})$, p_i is the last entry of $\mathbb{U}_i$, and q_i is the last element of $\mathbb{L}_i^{-1}\left(\frac{1}{\varepsilon_r} + \frac{k^2h^2}{12} + \frac{h^2}{6}\frac{1}{\varepsilon_r}\lambda_i\right)a_{N+1}$.

Otherwise, multiplying C_x^{-1} on both sides of Equation (33), we have

$$\begin{aligned} &2TL_1C_x\bar{u}_{:,N} + (2h\eta I_{M+2} + TL_2)C_x\bar{u}_{:,N+1} \\ =&2h\eta g + T\left(h^2F_{:,N+1} + \frac{h^4}{12}\Delta F_{:,N+1} - \eta\frac{h^3}{3}(f_y)_{:,N+1}\right). \end{aligned} \tag{36}$$

Combing (35) and (36), it follows

$$\begin{aligned} &\left(2h\eta C_x + TL_2C_x - 2TL_1C_xP^{-1}Q\right)\bar{u}_{:,N+1} \\ =&2h\eta g + T\left(h^2F_{:,N+1} + \frac{h^4}{12}\Delta F_{:,N+1} - \eta\frac{h^3}{3}(f_y)_{:,N+1}\right) - 2TC_x\mathbb{L}_i^{-1}P^{-1}\bar{F}_{:,N}. \end{aligned} \tag{37}$$

4. Fast High-Order Schemes for the Scattering from Finite Array of Cavities

In this section, we present fast algorithms to solve the electromagnetic scattering from the finite array of large cavities in the TE case. Consider the electromagnetic scattering from the finite array of large cavities $\Omega_1, \Omega_2, \ldots, \Omega_n$ embedded in an infinite ground plane. The geometry of the finite array of large cavities is shown in Figure 2. Assume the walls $S_l, l = 1, 2, \ldots, n$ of the cavities and the ground plane Γ_c are perfect electric conductors. Γ_l is the aperture of the cavity Ω_l separately. The half-space above the ground plane is filled with a homogeneous medium characterized by its dielectric permittivity ε_0 and magnetic permeability μ_0. The interior of the finite array of large cavities is filled with the nonmagnetic material with the relative dielectric permittivity $\varepsilon_r^{(l)}$ respectively.

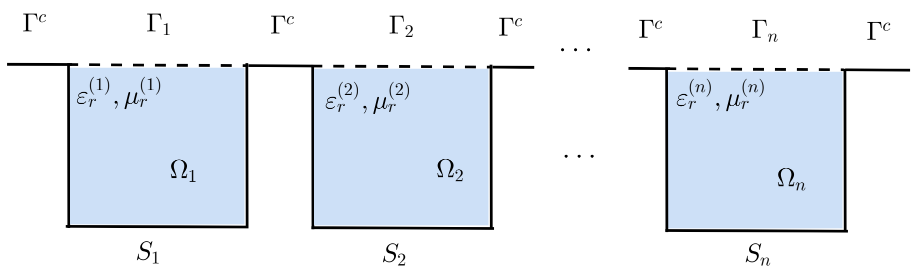

Figure 2. The geometric model of the finite array of cavities.

For the TE polarization case, Maxwell equations are reduced to the Helmholtz equations with Neumann boundary conditions. To reduce the scattering problem into bounded domain $\Omega_l, l = 1, 2, \ldots, n$, we need to obtain the boundary conditions on Γ_l. Rewrite the Helmholtz equation as

$$\begin{aligned} &\frac{1}{\varepsilon_r^{(l)}} \triangle u^{(l)} + k_0^2 u^{(l)} = 0, \quad &&\text{in } \Omega_l, \\ &\frac{1}{\varepsilon_r^{(l)}} \frac{\partial u^{(l)}}{\partial n} = 0, &&\text{on } S_l \cup \Gamma^c. \end{aligned} \tag{38}$$

Based on Equation (14), it follows that

$$u = T \frac{1}{\varepsilon_r} \left(\frac{\partial u}{\partial n} \right) + g(x), \text{ on } \bigcup_{l=1}^{n} \Gamma_j. \tag{39}$$

Extend $\frac{\partial u^{(l)}}{\partial n}$ to the whole x-axis by

$$\frac{\partial \tilde{u}^{(l)}}{\partial n} = \begin{cases} \dfrac{\partial u^{(l)}}{\partial n}, & x \in \Gamma_l, \\ 0, & x \in \mathbb{R} \setminus \Gamma_l. \end{cases}$$

For the total magnetic field $\frac{\partial u}{\partial \mathrm{n}}$, we have its x-axis extension

$$\frac{\partial \tilde{u}}{\partial n} = \begin{cases} \dfrac{\partial u^{(l)}}{\partial n}, & x \in \Gamma_l, \\ 0, & x \in \Gamma^c. \end{cases}$$

We have the following relationship

$$\tilde{u} = \tilde{u}^{(1)} + \tilde{u}^{(2)} + \cdots + \tilde{u}^{(l)} + g^{(l)}, \text{ on } \Gamma \cup \Gamma^c,$$

where $g^{(l)} = 2e^{\mathrm{i}\alpha x^{(l)}}$. The transparent boundary condition (39) can be rewritten as

$$\tilde{u} = T \frac{1}{\varepsilon_r^{(1)}} \left(\frac{\partial \tilde{u}^{(1)}}{\partial n} \right) + T \frac{1}{\varepsilon_r^{(2)}} \left(\frac{\partial \tilde{u}^{(2)}}{\partial n} \right) + \cdots + T \frac{1}{\varepsilon_r^{(n)}} \left(\frac{\partial \tilde{u}^{(n)}}{\partial n} \right) + g^{(l)}. \tag{40}$$

Therefore, the electromagnetic scattering from the finite array of large cavities in the TE polarization can be described as follows,

$$
\begin{aligned}
&\frac{1}{\varepsilon_r^{(l)}}\triangle u^{(l)} + k_0^2 u^{(l)} = 0, && \text{in } \Omega_l,\\
&\frac{1}{\varepsilon_r^{(l)}}\frac{\partial u^{(l)}}{\partial n} = 0, && \text{on } S_l \cup \Gamma^c,\\
&u^{(l)} = T\frac{1}{\varepsilon_r^{(l)}}\left(\frac{\partial \tilde{u}^{(l)}}{\partial n}\right) + \sum_{\substack{i=1\\ i\neq l}}^{n} T\frac{1}{\varepsilon_r^{(i)}}\left(\frac{\partial \tilde{u}^{(i)}}{\partial n}\right) + g^{(l)}, && \text{on } \Gamma_l.
\end{aligned}
\tag{41}
$$

The Fast Algorithm for the Scattering by a Finite Array of Cavities

Consider the second-order discretization of the transparent boundary condition on Γ

$$
u_{:,N+1}^{(l)} = \frac{1}{\varepsilon_r^{(l)}} T\frac{u_{:,N+2}^{(l)} - u_{:,N}^{(l)}}{2h} + \sum_{j=1, j\neq l}^{n} \frac{1}{\varepsilon_r^{(j)}} T\frac{u_{:,N+2}^{(j)} - u_{:,N}^{(j)}}{2h} + g^{(l)}, \quad \text{on } \Gamma_l. \tag{42}
$$

We rewrite (42) as matrix form

$$
2hu_{:,N+1}^{(l)} - \frac{1}{\varepsilon_r^{(l)}} T\left(u_{:,N+2}^{(l)} - u_{:,N}^{(l)}\right) - \sum_{j=1, j\neq l}^{n} \frac{1}{\varepsilon_r^{(j)}} T\left(u_{:,N+2}^{(j)} - u_{:,N}^{(j)}\right) = 2hg^{(l)}, \quad \text{on } \Gamma_l. \tag{43}
$$

On each aperture $\Gamma^{(l)}$, we have the following second-order approximation according to Equation (20)

$$
\begin{aligned}
&\left(\frac{1}{\varepsilon_r^{(l)}}\left(A_x - \frac{2}{h^2} I_{M+2}\right) + k_0^2\right) u_{:,N+1}^{(l)} + \frac{1}{\varepsilon_r^{(l)}}\frac{1}{h^2} u_{:,N}^{(l)} + \frac{1}{\varepsilon_r^{(l)}}\frac{1}{h^2} u_{:,N+2}^{(l)}\\
=&F_{:,N+1}^{(l)}, l = 1, 2, \dots, n.
\end{aligned}
\tag{44}
$$

Multiplying C_x^{-1} on both sides of (44), we have

$$
\left(\frac{1}{\varepsilon_r^{(l)}}\left(\Lambda - \frac{2}{h^2} I_{M+2}\right) + k_0^2\right) \bar{u}_{:,N+1}^{(l)} + \frac{1}{\varepsilon_r^{(l)}}\frac{1}{h^2} \bar{u}_{:,N}^{(l)} + \frac{1}{\varepsilon_r^{(l)}}\frac{1}{h^2} \bar{u}_{:,N+2}^{(l)} = \bar{F}_{:,N+1}^{(l)}. \tag{45}
$$

Denoting $J_1^{(l)} = \frac{1}{\varepsilon_r^{(l)}}\left(\Lambda - \frac{2}{h^2} I_{M+2}\right) + k_0^2$, $J_2^{(l)} = \frac{1}{\varepsilon_r^{(l)}}\frac{1}{h^2}$, we have

$$
\begin{aligned}
&\left(2hC_x + \frac{1}{\varepsilon_r^{(l)}} TC_x {J_2^{(l)}}^{-1} J_1^{(l)}\right) \bar{u}_{:,N+1}^{(l)} + 2\frac{1}{\varepsilon_r^{(l)}} TC_x \bar{u}_{:,N}^{(l)}\\
&+ \sum_{j=1, j\neq l}^{n} \left(T\frac{1}{\varepsilon_r^{(j)}} C_x {J_2^{(j)}}^{-1} J_1^{(j)} \bar{u}_{:,N+1}^{(j)} + 2\frac{1}{\varepsilon_r^{(j)}} TC_x \bar{u}_{:,N}^{(j)}\right)\\
=&\ 2hg^{(l)} + \sum_{j=1}^{n} TC_x {J_2^{(j)}}^{-1} F_{:,N+1}^{(j)}.
\end{aligned}
\tag{46}
$$

We apply the fast algorithm in each cavity Ω_l, and obtain

$$
P^{(l)} \bar{u}_{:,N}^{(l)} + Q^{(l)} \bar{u}_{:,N+1}^{(l)} = \tilde{F}^{(l)}, \ l = 1, 2, \dots, n, \tag{47}
$$

where

$$
\begin{aligned}
&P^{(l)} = \operatorname{diag}\left(p_1^{(l)}, p_2^{(l)}, \dots, p_{M+2}^{(l)}\right), Q^{(l)} = \operatorname{diag}\left(q_1^{(l)}, q_2^{(l)}, \dots, q_{M+2}^{(l)}\right),\\
&\tilde{F}^{(l)} = \left(\tilde{f}_{0,N}^{(l)}, \tilde{f}_{1,N}^{(l)}, \dots, \tilde{f}_{M+1,N}^{(l)}\right)^T.
\end{aligned}
$$

Combining (46) and (47) yields

$$\begin{aligned}
&\left(2hC_x + \frac{1}{\varepsilon_r^{(l)}} TC_x J_2^{(l)^{-1}} J_1^{(l)} - 2\frac{1}{\varepsilon_r^{(l)}} TC_x P^{(l)^{-1}} Q^{(l)}\right) \bar{u}^{(l)}_{:,N+1} \\
&+ \sum_{j=1, j\neq l}^{n} \left(\frac{1}{\varepsilon_r^{(j)}} TC_x J_2^{(j)^{-1}} J_1^{(j)} - 2\frac{1}{\varepsilon_r^{(j)}} TC_x P^{(j)^{-1}} Q^{(j)}\right) \bar{u}^{(j)}_{:,N+1} \\
=& 2hg^{(l)} + \sum_{j=1}^{n} \frac{1}{\varepsilon_r^{(j)}} T \left(J_2^{(j)^{-1}} \bar{F}^{(j)}_{:,N+1} + 2C_x P^{(j)^{-1}} \tilde{F}^{(j)} \right).
\end{aligned} \tag{48}$$

Therefore, we can derive the global system for the scattering problem from the finite array of large cavities in TE polarization

$$\begin{pmatrix} A_{11} & A_{12} & \cdots & A_{1n} \\ A_{21} & A_{22} & \cdots & A_{2n} \\ \vdots & \vdots & \ddots & \vdots \\ A_{n1} & A_{n2} & \cdots & A_{nn} \end{pmatrix} \begin{pmatrix} \bar{u}^{(1)}_{:,N+1} \\ \bar{u}^{(2)}_{:,N+1} \\ \vdots \\ \bar{u}^{(n)}_{:,N+1} \end{pmatrix} = \begin{pmatrix} b_1 \\ b_2 \\ \vdots \\ b_n \end{pmatrix}, \tag{49}$$

where

$$\begin{aligned}
A_{ii} &= 2hC_x + \frac{1}{\varepsilon_r^{(i)}} TC_x J_2^{(i)^{-1}} J_1^{(i)} - 2\frac{1}{\varepsilon_r^{(i)}} TC_x P^{(i)^{-1}} Q^{(i)}, \\
A_{ij} &= \frac{1}{\varepsilon_r^{(j)}} TC_x J_2^{(j)^{-1}} J_1^{(j)} - 2T\frac{1}{\varepsilon_r^{(j)}} C_x P^{(j)^{-1}} Q^{(j)}, \\
b_i &= 2hg^{(i)} + \sum_{j=1}^{n} \frac{1}{\varepsilon_r^{(j)}} TC_x \left(J_2^{(j)^{-1}} \bar{F}^{(j)}_{:,N+1} + 2P^{(j)^{-1}} \tilde{F}^{(j)} \right), \\
& i = 1, 2, \ldots, n, \ j = 1, 2, \ldots, n.
\end{aligned}$$

Similarly, we can apply the fast algorithm for the fourth-order scheme. Then we can derive the final fourth-order system on the apertures, which has the same expression as (49), where

$$\begin{aligned}
A_{ii} &= \left(2h\eta + TL_2^{(i)}\right) C_x - 2TL_1^{(i)} C_x (P^{(i)})^{-1} Q^{(i)}, \\
A_{ij} &= TL_2^{(i)} C_x - 2TL_1^{(i)} C_x (P^{(j)})^{-1} Q^{(j)}, \\
b_i &= 2h\eta g^{(i)} + \sum_{j=1}^{n} T \left(h^2 F^{(j)}_{:,N+1} + \frac{h^4}{12} \Delta F^{(j)}_{:,N+1} - \eta \frac{h^3}{3} (f_y)^{(j)}_{:,N+1} \right) \\
&\quad - \sum_{j=1}^{n} 2TC_x (P^{(j)})^{-1} (\mathbb{L}_i^{(i)})^{-1} \tilde{F}^{(j)}_{:,N}, i = 1, 2, \ldots, n, \ j = 1, 2, \ldots, n.
\end{aligned}$$

5. Numerical Experiments

In this section, a variety of numerical experiments are demonstrated to examine the efficiency of the proposed fast high-order algorithms for electromagnetic scattering by the finite array of cavities with high wave numbers. All the examples are computed with double precision and are performed on a desktop with an Intel(R) Core(TM) i5-9400F CPU, 2.90 GHz, and 16.00 GB memory. We present errors in L^∞ norm and estimate the convergence order by

$$r = \frac{\log(\|e_{h_1}\|_\infty / \|e_{h_2}\|_\infty)}{\log(h_1/h_2)}.$$

5.1. Example 1

We consider a rectangular cavity of 1 m wide and 1 m deep. The exact solution is selected as

$$u = \cos(k_0 x)\sin((k_0 + \pi/2)y), \quad (x, y) \in [0, 1] \times [-1, 0].$$

The source term $f(x)$ is derived from the (14) by changing the wave number and the relative permittivity. The errors and the convergence rates for the cavity filled with different materials are given in Tables 1–3. It is shown that the convergence orders for the schemes are two and four respectively. The numerical solution and the error of the proposed schemes for Example 1 with $k_0 = 16\pi\text{m}^{-1}$, $h = 1/1024$ m are represented in Figure 3.

Table 1. Numerical convergence orders of the second-order fast algorithm with $k_0 = 8\pi\text{m}^{-1}$, $\varepsilon_r = 4 + \text{i}$.

h	$e_\infty(\Gamma)$	Order	$e_\infty(\Omega)$	Order	CPU Time (s)
1/16	2.0281×10^{-1}		9.7386×10^{-2}		0.0080
1/32	4.6314×10^{-2}	2.1306	4.4007×10^{-2}	1.1460	0.0982
1/64	1.1937×10^{-2}	1.9560	1.3852×10^{-2}	1.6676	0.0200
1/128	3.0142×10^{-3}	1.9856	3.4765×10^{-3}	1.9944	0.0317
1/256	7.5720×10^{-4}	1.9931	8.7693×10^{-4}	1.9871	0.0894

Table 2. Numerical convergence orders of the fourth-order fast algorithm with $k_0 = 8\pi\text{m}^{-1}$, $\varepsilon_r = 4 + \text{i}$.

h	$e_\infty(\Gamma)$	Order	$e_\infty(\Omega)$	Order	CPU Time (s)
1/16	2.9375×10^{-1}		1.6377×10^{-1}		0.0382
1/32	1.9114×10^{-2}	3.9419	1.1956×10^{-2}	3.7758	0.0561
1/64	1.3079×10^{-3}	3.8694	1.1329×10^{-3}	3.3997	0.0737
1/128	8.4704×10^{-5}	3.9486	8.0131×10^{-5}	3.8215	0.1400
1/256	5.3553×10^{-6}	3.9834	5.2272×10^{-6}	3.9382	0.6564

Table 3. Numerical convergence orders of the fourth-order fast algorithm with $k_0 = 16\pi\text{m}^{-1}$, $\varepsilon_r = 4 + \text{i}$.

h	$e_\infty(\Gamma)$	Order	$e_\infty(\Omega)$	Order	CPU Time (s)
1/64	2.1762×10^{-2}		1.4052×10^{-2}		0.0478
1/128	1.4300×10^{-3}	3.9277	1.2347×10^{-3}	3.5086	0.0908
1/256	9.1459×10^{-5}	3.9668	8.6201×10^{-5}	3.8403	0.5833
1/512	5.7521×10^{-6}	3.9910	5.6021×10^{-6}	3.9437	5.4535
1/1024	3.6003×10^{-7}	3.9979	3.5557×10^{-7}	3.9778	66.1697

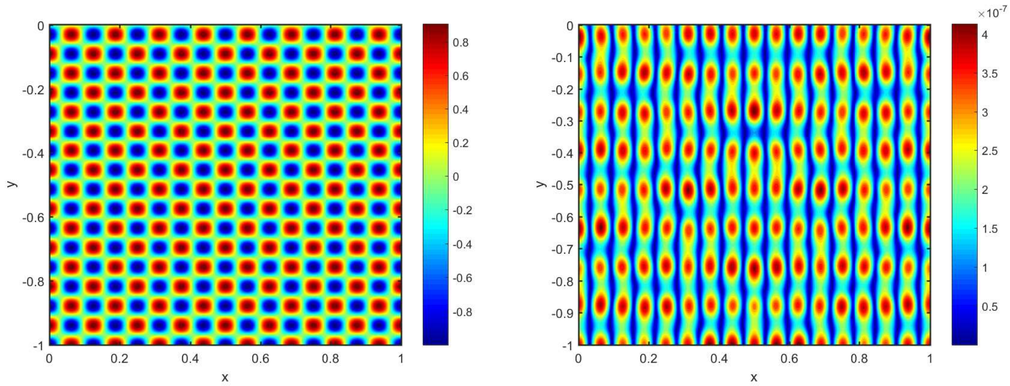

Figure 3. The real part of the numerical solution (**left**) and the absolute error plot (**right**) for the empty cavity with $k_0 = 16\pi\mathrm{m}^{-1}$, $h = 1/1024$ m.

5.2. Example 2

We examine the validity of the proposed algorithms for the scattering problem from the single cavity further. We consider a 1 m wide and 0.25 m deep cavity scattering illuminated by a 300-MHz TE plane wave. The example was tested by Du's results [30]. The physical parameter backscatter RCS can be calculated as follows. Let $\sigma(\theta) = \frac{4}{k_0}|P(\theta)|^2$, where θ is the observation angle and P is the far-field coefficient given by

$$P(\theta) = \frac{k_0}{2} \sin\theta \int_\Gamma \mathrm{e}^{(\mathrm{i}k_0 x \cos\theta)} u dx.$$

When the incident angle is the same as the observation direction, the backscatter RCS is defined by

$$\text{Backscatter RCS}(\theta) = 10 \log_{10} \sigma(\theta) dB.$$

Figures 4 and 5 display the magnitude and RCS of cavities filled with the homogeneous media $\varepsilon_r = 1$ and $\varepsilon_r = 4 + \mathrm{i}$ in TE polarization, where 'o' denotes the solutions derived in [30]. Clearly, the numerical results coincide with those of Du's method. Moreover, we can see from Table 4 that the fast algorithm remarkably reduces the computational time.

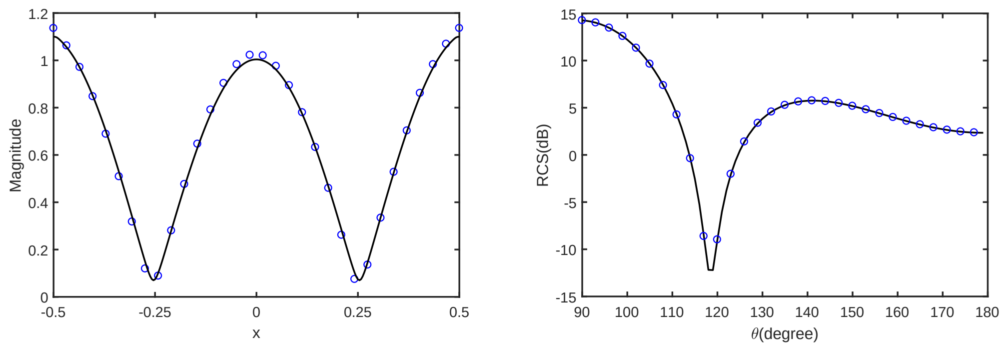

Figure 4. The magnitude of the aperture fields at normal incidence (**left**) and backscatter RCS (**right**) in TE polarization with $k_0 = 2\pi\mathrm{m}^{-1}$, $\varepsilon_r = 1, h = 1/256$ m, 'o': the solutions derived in [30], '-': our results.

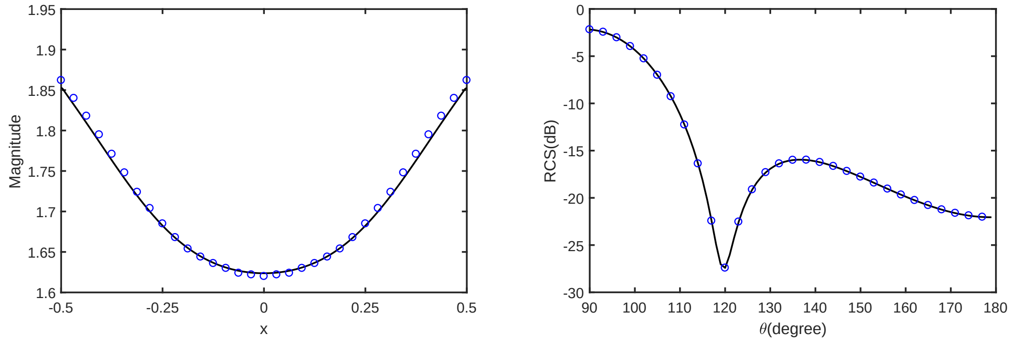

Figure 5. The magnitude of the aperture fields at normal incidence (**left**) and backscatter RCS (**right**) in TE polarization with $k_0 = 2\pi\mathrm{m}^{-1}$, $\varepsilon_r = 4 + \mathrm{i}, h = 1/256$ m, 'o': the solutions derived in [30], '-': our results.

Table 4. The comparison of the computational time for the proposed normal and fast fourth-order scheme.

h	**CPU Time of Fourth-Order Scheme (s)**	**CPU Time of Fast Fourth-Order Scheme (s)**
1/128	0.0211	0.0083
1/256	0.3503	0.0544
1/512	1.3928	0.2142
1/1024	8.1006	1.2517
1/2048	out of memory	10.7882

5.3. Example 3

In order to address the electromagnetic scattering from the finite array of large cavities, we first consider a two-cavity scattering problem by two identical rectangular cavities of 1 m wide and 1 m deep. It is investigated that the farther the distance between the finite array of cavities, the smaller the coupling impact of each other, see [31] for details. Therefore, for high wave number problems, we consider the distance between cavities is equal to the width of the cavity. Backscatter RCS comparisons for the scattering from two cavities in TE polarization are displayed in Figures 6 and 7. The cavities are filled with $\varepsilon_r = [\varepsilon_r^{(1)}, \varepsilon_r^{(2)}] = [2, 2]$, complex material $\varepsilon_r = [\varepsilon_r^{(1)}, \varepsilon_r^{(2)}] = [2 + 0.1\mathrm{i}, 2 + 0.1\mathrm{i}]$, and $\varepsilon_r = [\varepsilon_r^{(1)}, \varepsilon_r^{(2)}] = [2 + 10\mathrm{i}, 2 + 10\mathrm{i}]$ respectively. We can see that the backscatter RCS of cavities filled with a lossy medium is lower than that of cavities filled with a lossless medium. Moreover, it is observed that the backscatter RCS of cavities decreases with the increase of the imaginary part of the medium. Therefore, the RCS can be reduced by filling the cavity with the absorbing material coating.

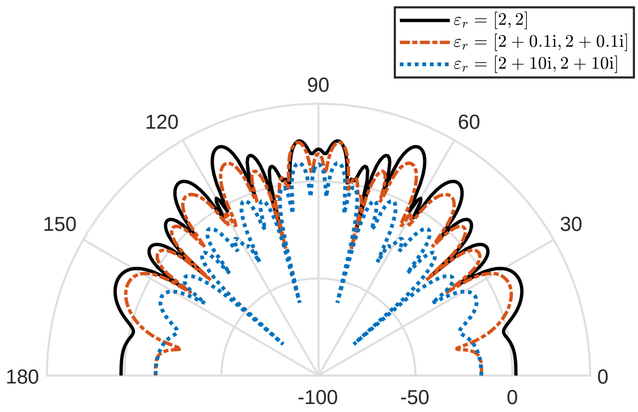

Figure 6. The backscatter RCS by two cavities in TE polarization with $k_0 = 4\pi\mathrm{m}^{-1}$ on 256×256 meshes for the media $[2, 2]$, $[2 + 0.1\mathrm{i}, 2 + 0.1\mathrm{i}]$ and $[2 + 10\mathrm{i}, 2 + 10\mathrm{i}]$.

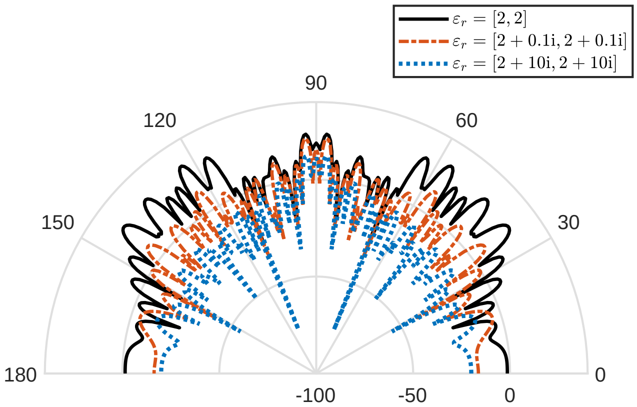

Figure 7. The backscatter RCS by two cavities in TE polarization with $k_0 = 8\pi m^{-1}$ on 512×512 meshes for the media $[2, 2]$, $[2 + 0.1\mathrm{i}, 2 + 0.1\mathrm{i}]$ and $[2 + 10\mathrm{i}, 2 + 10\mathrm{i}]$.

5.4. Example 4

We consider a three-cavity scattering problem by three identical rectangular cavities that are 1 meter wide and 0.5 meters deep. The distance between cavities is equal to the width of the cavity. We plot the contour for the real part of the magnetic field with $k_0 = 8\pi \mathrm{m}^{-1}$ and $k_0 = 16\pi \mathrm{m}^{-1}$ for the media of $\varepsilon_r = 2.38 + 0.12\mathrm{i}$ at $\theta = \pi/3$ and $\theta = \pi/4$ in Figures 8 and 9.

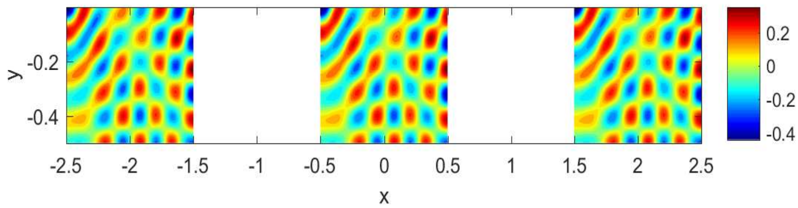

Figure 8. Contour for real part of the magnetic field by three empty cavities with $k_0 = 8\pi \mathrm{m}^{-1}$ of 512×256 mesh at $\theta = \pi/3$.

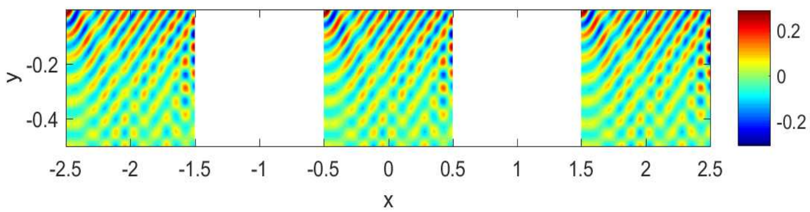

Figure 9. The real part of the magnetic field by three empty cavities with $k_0 = 16\pi \mathrm{m}^{-1}$ of 1024×512 mesh at $\theta = \pi/4$.

6. Conclusions

In this paper, we present fast high-order algorithms for solving the electromagnetic scattering from the finite array of cavities with large wave numbers in TE polarization. Compact second-order and fourth-order schemes are applied to discretize the magnetic field equation in TE polarization. The boundary conditions of the cavity arrays are decoupled by a new transparent boundary condition. The fast algorithm is based on the FFT-cosine transformation in the horizontal direction and the Gaussian elimination in the vertical direction. Numerical experiments validate the convergence order and the efficiency of the proposed fast high-order algorithms.

Author Contributions: Conceptualization, methodology, M.Z.; writing—original draft preparation, J.H.; writing—review and editing, N.Z.; funding acquisition, M.Z. All authors have read and agreed to the published version of the manuscript.

Funding: The research was supported by the Natural Science Foundation of Hebei Province (No. A2020502003) and the Fundamental Research Funds for the Central Universities (No. 2021MS115).

Institutional Review Board Statement: Not applicable.

Informed Consent Statement: Not applicable.

Data Availability Statement: Not applicable.

Conflicts of Interest: The authors declare no conflict of interest. The funders had no role in the design of the study; in the collection, analyses, or interpretation of data; in the writing of the manuscript, or in the decision to publish the results.

References

1. Wang, C.; Gan, Y. 2D cavity modeling using method of moments and iterative solvers. *J. Electromagn. Waves Appl.* **2003**, *17*, 1739–1740. [CrossRef]
2. Wood, W.; Wood, A. Development and numerical solution of integral equations for electromagnetic scattering from a trough in a ground plane. *IEEE T. Antenn. Propag.* **1999**, *47*, 1318–1322. [CrossRef]
3. Jin, J. *The Finite Element Method in Electromagnetics*, 2nd ed.; John Wiley and Sons: New York, NY, USA, 2002.
4. Liu, J.; Jin, J. A special higher order finite-element method for scattering by deep cavities. *IEEE Trans. Antennas Propag.* **2000**, *48*, 694–703.
5. Liu, J.; Jin, J. A highly effective preconditioner for solving the finite element-boundary integral matrix equation of 3-D scattering. *IEEE Trans. Antennas Propag.* **2002**, *50*, 1212–1221. [CrossRef]
6. Ross, D.; Volakis, J.; Anastassiu, H. Hybrid finite element-modal analysis of jet engine inlet scattering. *IEEE Trans. Antennas Propag.* **1995**, *43*, 277–285. [CrossRef]
7. Alavikia, B.; Ramahi, O. Hybrid finite-element-boundary integral algorithm to solve the problem of scattering from a finite and infinite array of cavities with stratified dielectric coating. *J. Opt. Soc. Am. A* **2011**, *28*, 1022–1031. [CrossRef] [PubMed]
8. Alavikia, B.; Ramahi, O. Coupling interactions in electromagnetic scattering from finite array of cavities with stratified dielectric coating. *J. Opt. Soc. Am. A* **2012**, *29*, 1132–1140. [CrossRef] [PubMed]
9. Ito, K.; Qiao, Z.; Toivanen, J. A fast preconditioned iterative algorithm for the electromagnetic scattering from a large cavity. *J. Sci. Comput.* **2012**, *53*, 435–450.
10. Bao, G.; Sun, W. A fast algorithm for the electromagnetic scattering from a large cavity. *SIAM J. Sci. Comput.* **2005**, *27*, 553–574. [CrossRef]
11. Ito, K.; Qiao, Z.; Toivanen, J. A domain decomposition solver for acoustic scattering by elastic objects in layered media. *J. Comput. Phys.* **2008**, *227*, 8685–8698. [CrossRef]
12. Zhao, M. A fast high order iterative solver for the electromagnetic scattering by open cavities filled with the inhomogeneous media. *Adv. Appl. Math. Mech.* **2013**, *5*, 235–257. [CrossRef]
13. Zhao, M.; Qiao, Z.; Tang, T. A fast high order method for electromagnetic scattering by large open cavities. *J. Comput. Math.* **2011**, *29*, 287–304. [CrossRef]
14. Zhao, M.; Zhu, N. A fast preconditioned iterative method for the electromagnetic scattering by multiple cavities with high wave numbers. *J. Comput. Phys.* **2019**, *398*, 108826. [CrossRef]
15. Schiavone, G.; O'Neill, K.; Paulsen, K. Scattering from groove patterns in a perfectly conducting surface. *J. Opt. Soc. Am. A* **1997**, *14*, 2212–2222. [CrossRef]
16. Van, T.; Wood, A. A time-domain finite element method for helmholtz equations. *J. Comput. Phys.* **2002**, *183*, 486–507. [CrossRef]
17. Li, P. A survey of open cavity scattering problems. *J. Comput. Math.* **2019**, *36*, 1–16. [CrossRef]
18. Xiang, Z.; Chia, T. A hybrid BEM/WTM approach for analysis of the EM scattering from large open-ended cavities. *IEEE Trans. Antennas Propag.* **2001**, *49*, 165–173. [CrossRef]
19. Li, P.; Wang, L.; Wood, A. Analysis of transient electromagnetic scattering from a three-dimensional open cavity. *SIAM J. Appl. Math.* **2015**, *75*, 1675–1699. [CrossRef]
20. Jiang, X.; Li, P.; Lv, J.; Zheng, W. An adaptive finite element method for the wave scattering with transparent boundary condition. *J. Sci. Comput.* **2017**, *72*, 936–956. [CrossRef]
21. Chen, Y.; Jiang, X.; Lai, J.; Li, P. A fast algorithm for the electromagnetic scattering from a large rectangular cavity in three dimensions. *J. Comput. Phys.* **2021**, *437*, 110331. [CrossRef]
22. Du, K.; Sun, W.; Zhang, X. Arbitrary high-order C^0 tensor product Galerkin finite element methods for the electromagnetic scattering from a large cavity. *J. Comput. Phys.* **2013**, *242*, 181–195. [CrossRef]
23. Mumtaz, F.; Ashraf, M.; Dai, Y. Numerical approach to approximate the electromagnetic scattering from random PEC cylinder placed below in dielectric half-space. *Optik* **2020**, *206*, 163751. [CrossRef]
24. Zhao, M.; Zhu, N.; Wang, L. Fast algorithms for the electromagnetic scattering by partly covered cavities. *J. Comput. Appl. Math.* **2021**, *40*, 7. [CrossRef]
25. Ammari, H.; Bao, G.; Wood, A. A cavity problem for maxwell's equations. *Meth. Appl. Anal.* **2002**, *9*, 249–260. [CrossRef]

26. Ammari, H.; Bao, G.; Wood, A. Analysis of the electromagnetic scattering from a cavity. *J. Jpn. J. Indust. Appl. Math.* **2002**, *19*, 301–310. [CrossRef]
27. Bao, G.; Zhang, W. An improved mode-matching method for large cavities. *IEEE Antennas Wirel. Propag. Lett.* **2005**, *4*, 393–396.
28. Li, P.; Wood, A. A two-dimensional helmhotlz equation solution for the multiple cavity scattering problem. *J. Comput. Phys.* **2013**, *240*, 100–120. [CrossRef]
29. Wu, X.; Zheng, W. An adaptive perfectly matched layer method for multiple cavity scattering problems. *Commun. Comput. Phys.* **2016**, *19*, 534–558. [CrossRef]
30. Du, K. Two transparent boundary conditions for the electromagnetic scattering from two-dimensional overfilled cavities. *J. Comput. Phys.* **2011**, *230*, 5822–5835. [CrossRef]
31. Uber, R. Time Domain Analysis of the Electromagnetic Scattering From Multiple Cavities Embedded in a Ground Plane. Ph.D. Thesis, Air Force Institute of Technology, Wright-Patterson AFB, OH, USA, 2016.